Case study comparisons of UK macro-tidal regime wave and current interaction processes; mesoscale wave model versus coastal buoy data.

Tamzin Palmer[1], Tom Stratton[2], Andrew Saulter[1], Edmund Henley[1]

1. **UK Met Office, FitzRoy Road, Exeter, EX1 3PB, tamzin.palmer@metoffice.gov.uk**
2. **Department of Physics, Lancaster University, Bailrigg, Lancaster, UK, LA1 4YW**

1. Introduction

1.1 Study Area

The effects of tidal currents on waves can be significant and as such the accurate prediction of wave-current interaction is important to any coastal wave forecasting model. Modern 3rd generation wave models are able to account for the effects of currents on waves. A number of studies have validated the models in both deep water and coastal areas (Hothuijsen and Tolman 1991, Ardhuin et al., 2012)

The primary source of energy input to the waves is the wind; this is the main variable that influences the development of the wave spectrum (Ardhuin 2012). The effect of currents on waves are second order and changes in the wave spectrum due to their influence may be hard to separate from the effect of variations in the wind speed and direction. For this reason, when assessing the effect of the addition of currents to the performance of a wave model, it is useful to use case studies. This paper presents the use of a discrete wavelet analysis to identify suitable case studies. Wavelet analysis decomposes time series into a number of approximate frequencies and enables the frequency corresponding to the tidal signal within the wave parameters to be identified. Cross correlation of the wavelet decomposition with the tidal time series is also demonstrated to be a useful way to validate the time-series over longer periods of time.

Around the UK there are a number of locations where tidal ranges vary by several metres and current speeds are often in excess of 2 m/s. One area of interest to UK wave forecasting is the English Channel, in particular near the Isle of Wight where significant tidal currents are observed in the central Channel. A strong tidal signal in the wave parameters is observed at the wave buoys around this region. This area has been chosen as one of the case studies examined in this paper. Strong tidal modulations in both significant wave height (Hs) and mean zero-upcrossing period (Tz) are observed by the Channel Coastal Observatory (CCO) wave buoy at Rustington. Another area of interest is the Bristol Channel. This estuary has a tidal range of up to 14m and tidal currents in excess of 2.5 m/s. The CCO Bideford wave buoy is located at the coast near to the entrance to the Bristol Channel. This has been chosen as a second case study area. The locations of the two study areas and the wave buoy locations used are shown in figure 1.

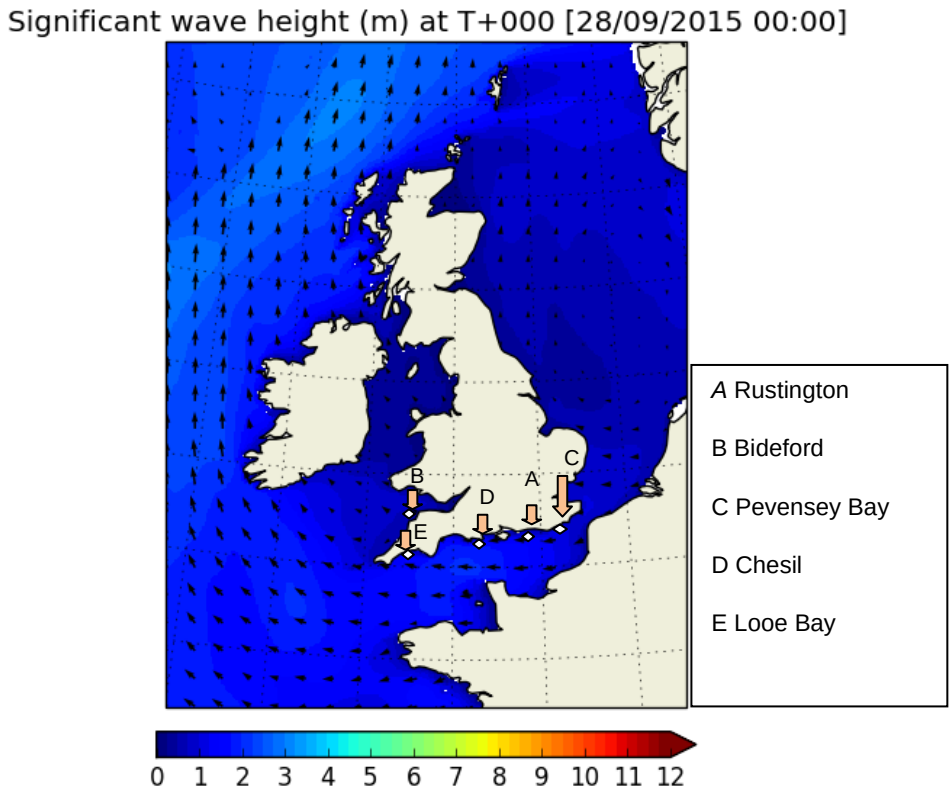

Figure 1 Output field for Hs showing the UK 4km model domain and validation locations

1.2 Wave-current interaction in coastal waters

Changes in water depth and ambient currents due to tides are known to alter the wave field through a number of processes. The amplitude, frequency and direction of a propagating wave may be altered by a current field (Hayes 1981, Hothuijsen and Tolman 1991). When waves propagate against an opposing current blocking may occur if the group speed of the waves becomes less than that of the current. In this case the wave steepness will often become large enough to induce wave breaking and dissipation of the wave energy (Ardhuin et al. 2012, Dodet et al., 2013). In some cases this can lead to the formation of extremely steep waves, for example in the Agulhas current (Hayes 1981, Schuman 1975, 1976). In the case of a following current the wavelength will increase and the wave height and steepness will decrease.

WAVEWATCH III solves the action density spectrum; wave energy is not conserved as waves propagate through the current field. This is due to the exchange of energy between the waves and the currents due to radiation stress (Longuet-Higgins and Stewart (1960. 1964). Action density is however conserved and the use of this quantity in place of the energy density spectrum allows the model to account for wave-current interactions (Tolman 2009).

Third generation wave models such as WAVEWATCH III also contain parameterizations to address the dissipation of wave energy due to whitecapping. These parameterizations are generally quasi linear with a coefficient that multiplies the frequency-directional power spectrum. This coefficient is usually proportional to the fourth power of the wave steepness (or can be higher), which will increase in the presence of an opposing current. The definition of steepness varies between parameterizations (Ardhuin et al., 2012).

Currents may also affect the local generation of waves. The speed and direction of a current may alter the effective fetch or the relative effect of the wind speed on the waves. This can lead to an increase in the wave height and peak frequency where the wind direction opposes the currents. WAVEWATCH III uses a parameterisation to account for the relative wind effect by using the difference between the two vector velocities (Tolman 2009).

Currents also alter the wave direction by refraction. Current induced refraction occurs by the same process as depth induced refraction: the wave turns towards the area with lower propagation speed of the crest. The wave speed, relative to a fixed point on the sea bed, will be affected by the ambient current as well as changes in the water depth (Holthuijsen 2007). Ardhuin et al., (2012) found that strong currents up wave of a wave buoy can lead to changes locally at the buoy. This is likely to be the case in the English Channel to the east of the Isle of Wight where strong currents occur in the central channel. It was also found that current refraction has a greater impact on swell than wind-sea waves (Ardhuin et al., 2012). Swell waves from the North Atlantic may propagate from west to east in the Channel along with locally generated wind-sea. It may be the case that current refraction effects are stronger when swell waves are present.

Currents in the ocean are never uniform across stream and therefore changes in the frequency and direction of waves will occur due to the across stream gradients in current speed. Focussing in the middle of current jets may also occur due to refraction. An extreme example of this is observed in the Agulhas current (Kunze 1985).

Changes in frequency are closely related to the Doppler Effect. The frequency of a wave moving in a frame of reference with the current is called the relative frequency or intrinsic frequency (denoted by σ). In a fixed frame of reference, for example relative to the sea-bed, the frequency is called the absolute frequency (denoted as ω). It is related to the relative frequency as (equation 1):

$$\boldsymbol{\omega = \sigma + KU_n} \quad (1)$$

Where U_n is the component of the current in the wave direction and K is the wave number (Holthuijsen 2007). In shelf seas, such as the English Channel in the UK, currents and depths are unsteady and inhomogeneous, which means that both the relative and absolute frequency will change (Tolman 1990).

In the case of a current or water depth that varies horizontally and in time, the rate of change of the relative frequency is given by equation 2:

$$\frac{d\sigma}{dt} = C\sigma = \frac{\partial\sigma}{\partial d}\left(\frac{\partial d}{\partial t} + U\frac{\partial d}{\partial s}\right) - C_g k\frac{\partial U_n}{\partial n} \quad (2)$$

(Holthuijsen 2007)

Where t is time, d is depth, s is the streamline of the current and n is the wave orthogonal (normal to the crest). The absolute frequency and wave number will change in accordance with the relative frequency as shown in equation 1.

2 Methods

2.1 Model set-up

The Met Office has used the WAVEWATCH III (3.14) ocean surface model for all its operational model configurations since 2008. It is a community model initially developed by Hendrik Tolman (Tolman 1991), it is now under continual development by the wave modelling community. The operational Met Office version of the model operates a second-order advection scheme (Li 2008) and a rotated grid for the UK 4km model used in this study. Wind forcing is taken from Met Office global UM analysis fields. The UK 4km model was run for 2012. Two model runs were carried out, a control run with wind forcing only and a run for the same time period with an identical model configuration which included the addition of an hourly current field from the 7km Atlantic Margin Model (AMM7).

The Atlantic Margin Model (AMM7) is a coupled hydrodynamic-ecosystems model, nested into the Met Office global Forecast Ocean Assimilation Model (FOAM) configuration (O'Dea et al., 2012). The FOAM AMM system is run daily and produces 3D analyses and 6 day forecasts of ocean currents, traces and several biogeochemical and optical quantities. The AMM non-tidal boundary conditions are taken from NEMO (Nucleus for European Modelling of the Ocean). Surface forcing for NEMO is taken from the Met Office NWP model this includes: heat, moisture, wind speed and surface pressure. Tidal forcing on the open boundary is via a Flather radiation boundary condition (Flather 1976) and through the inclusion of an equilibrium tide

2.2. Isolating modulations due to tidal currents in a time series using a discrete wavelet analysis.

For studies of real-world conditions, one of the challenges faced, when validating the introduction of a current field to a model, is identifying locations and instances where the currents affect the wave field to a similar, or larger, extent than variations in the wind field. Wind induced modulations in the wave parameters, over a similar time scale as those caused by tides (approximately 12 hours), often make it difficult to analyse the extent of the modulations due to tidal effect alone. This in turn makes it difficult to validate the performance of a wave model that is coupled to a current model. In this study a wavelet analysis is used to address this problem.

In order to isolate periods of strong modulation due to tidal effects as far as possible, a discrete wavelet analysis was carried out on the wave model time series for each wave buoy

location. The wavelet analysis can be used to analyse a time series that contain non-stationary power at a number of different frequencies (Daubechies 1990). The time series must contain equal time spacing and must be continuous. A time series of wave parameters generated by a wave model over a period of 6 – 12 months, with an hourly or half hourly output, is suitable for such an analysis.

For a discrete wavelet analysis an orthogonal wavelet function is used. The number of convolutions at each wavelet scale is proportional to the width of the wavelet basis at that scale. A finite number of wavelet scales are used, allowing a particular frequency to be isolated and the power in that frequency at a given time to be calculated. Discrete wavelet analysis is useful for signal processing as it provides the most compact representation of the signal (Torrence and Compo 1998).

The discrete wavelet analysis uses the wavelet function (ψ) and the scaling function (ω) as high and low pass filters respectively. Both functions have a finite temporal width that can be scaled to filter for different frequencies. The wavelet function is dilated according to a dyadic scale (n), where each level in the decomposition is increased by 2^n. ψ_n (high pass filter) calculates the coefficients cD_n for the frequency at scale n, while ω_n acts as a low pass filter and calculates the approximation coefficients (cA_n) for all the frequencies below ψ_n. The approximation coefficients (cA_n) are then passed on to the next dilation scale (2^{n+1}), ψ_{n+1} and ω_{n+1} are then used to calculate cD_{n+1} and cA_{n+1} respectively. Figure 2 shows an overview of the process. At any level the coefficients can be upsampled to reconstruct the original signal; this allows the signal power at each of the dilation scales to be calculated. The process allows the original signal to be perfectly reconstructed from the coefficients. Each of the reconstructed detail levels (high pass wavelet function) can be added together along with the reconstructed low pass filter to obtain the original signal.

The wavelet function should be chosen according to the type of features present in the time series. A symlet (close to symmetrical) was chosen, as this has a form similar to modulations in a time series of wave parameters caused by the effects of the tide (figure 3). A wavelet is not perfectly located in time and space; this means that only an approximate frequency can be calculated from the central frequency of the wavelet and the scale factor. The central frequency of the wavelet was also chosen to allow an approximate frequency as close to the semi-diurnal (M2) tidal signal as possible. At the second dilation level the 'Sym 5 ' wavelet (see figure 3) was found to be both the best match to the features in the data and also allowed a 12 hour approximate frequency to analysed (equation 4).

$$Fa = \frac{Fc}{s \times \Delta} \quad (4)$$

where Fa is the approximate frequency, Fc central frequency, $s = 2^n$ and Δ is the sample width of the data set.

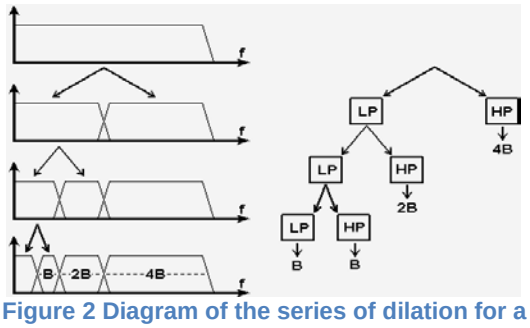

Figure 2 Diagram of the series of dilation for a multi-level discrete wavelet analysis.

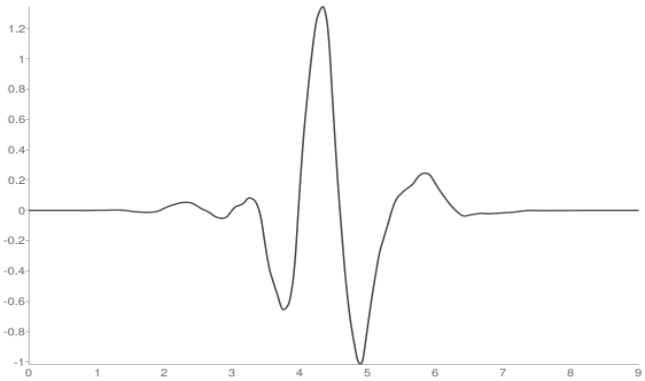

Figure 3 'Sym 5' symlet

While the wavelet can be used to identify power in the time series at approximately the same frequency as the diurnal tidal signal, it is not possible to be sure that the modulations are due to the effects of the currents alone. It is possible that the tidal signal in the wave parameter time series is 'contaminated' by variations caused by fluctuations in the forcing wind at the same frequency. In order to select time periods when the contamination of the tidal signal by the wind forcing is minimised, two model runs were analysed. A control run of the wave model was made with only a wind field as forcing; the run was then repeated with the addition of the current fields. A wavelet analysis was carried out on both model outputs and the signal power compared at the12 hour period. During time periods where strong signal power was seen in the wavelet analysis from the model run that included a current field and in the observations, while negligible signal power was seen for the model run without a current field, the assumption was made that the modulations in the wave parameters were due to the effect of tidal currents.

An example is shown in Figure 4, where a wavelet analysis was carried out for the Rustington wave buoy. Figure 4a) shows the original Hs time series for the observations, the model with currents and the control model. The wavelet filter for 12 hours (level2 for the model and level 3 for the wave buoy which measures at half hourly intervals), is shown in 4b). Figure 4c shows the average signal power of the 12 hour wavelet, reconstructed over a 12 hour window (4c); in this figure it can be seen at a glance where there is a large difference between the observations and the control model run. A stronger signal in the control model indicates that modulations are occurring due to other processes such as the wind at a 12 hour frequency. Where the signal power for the control model run is low, but high for the observations, this indicates that the currents have had a dominant effect on changes in the wave field at a 12 hour frequency. Comparing the wavelet 12 hour filter for the observations with the model run with currents it can be seen that the modulation amplitude 4b) and the signal power 4c) are often similar for the observations and the model. In general the current induced modulations predicted by the wave model with currents are usually in reasonable agreement with the model at this location.

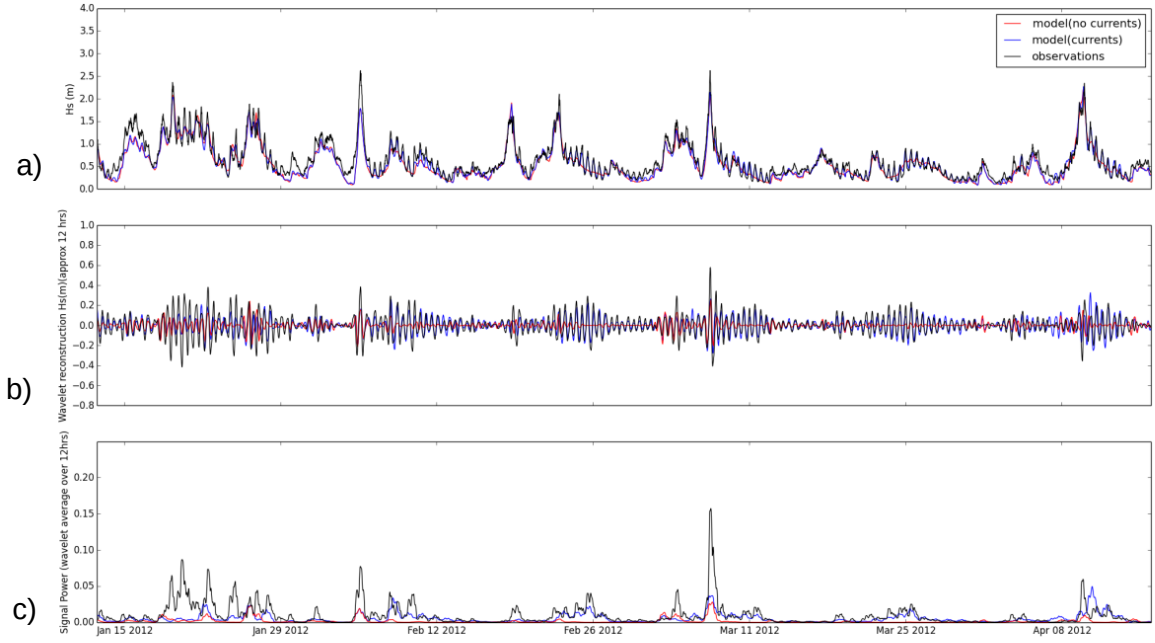

Figure 4 Example of wavelet analysis at Rustigton a) Orginal Hs b) wavelet 12 hour filter c) Signal power averged over 12 hours

3. Results

3.1 Cross correlation between wave and the tidal signal.

Reconstructed high pass wavelet signals for Hs and Tz at the 12 hour frequency were compared with the tidal modulations in sea surface height at each wave buoy site for a 3 month period, from 2012/01/02 to 2012/04/01. A lagged cross correlation analysis was used to determine the maximum Pearson Correlation between the signals and the time difference at which this occurred. The results are shown in table 1 for (respectively) observations, model with currents and the control run without currents.

At Rustington the observed modulations in Hs and Tz both correlate strongly with the sea surface height, the maximum Hs and Tz occurred at high tide with the minimum values at low tide. The observation peak correlation is also in phase with the model with currents at Rustington and of a similar order. In contrast, the control run shows no correlation with the sea surface height. This is a strong indication that the addition of a current field improves the ability of the model to represent the tidal processes influencing the wave field and that the model is able to qualitatively represent the dominant wave-current interactions at this location. Since tidal elevations are not included in the wave model the results indicate that the effects on the wave field due to wave-current interactions are predominantly responsible for the tidal signal observed at Rustington.

Table 1 Maximum Pearson Correlation Coefficient between the sea surface and the wavelet anaylsis at 12 hours.

Location	Wave parameter	Pearson Correlation Coefficient (Obs, Model, Model – no currents)	Lag behind SSH (Obs, Model, Model – no currents)
Rustington	**Hs**	**0.637, 0.623 , 0.005**	**12, 12 , 12**
	Tz	**0.645, 0.559 , 0.113**	**0, 0, 4**
Bideford	**Hs**	**0.706, 0.501 , 0.014**	**8, 9 ,10**
	Tz	**0.666, 0.266, 0.146**	**6, 5, 1**
Looe Bay	**Hs**	**0.066, 0.060 , 0.024**	**5, 9, 6**
	Tz	**0.389, 0.256, 0.109**	**5, 2, 4**
Pevensey	**Hs**	**0.373, 0.341, 0.062**	**0, 0, 5**
	Tz	**0.449, 0.514, 0.101**	**1, 0, 4**
Chesil	**Hs**	**0.519, 0.170, 0.098**	**3, 3, 4**
	Tz	**0.580, 0.188, 0.056**	**3, 6, 9**

At other locations in the English Channel to the east and west of the Isle of Wight, the correlation between the modulations and the sea surface height is lower than Rustington. Current speeds are often in excess of 2m/s in the central Channel near the Isle of Wight (see figure 5) , but reduce to the east and west. There is also a lag between the modulations and the sea surface height that increases to the west of Rustington. In general the tidal signal in the wave field is weaker at the other channel locations than at Rustington. This is evident in the correlation values between the SSH and the wavelet 12 hour filter for the observations. This weaker tidal signal is reflected in the model with currents at most locations. The exception to this is at Chesil where the correlation is notably higher for the observations. The tidal range at Chesil is a maximum of about 4m, which is similar to Rustington. The bathymetry around or approaching Chesil may result in some wave focussing occurring with changes in the water depth, which is not accounted for in this wave model. There are also some areas of faster currents near the Chesil buoy that may not be well resolved by the AMM7 model. This is speculative however and should be investigated further when water

levels are added to the model. In all cases the model with currents is closer in terms of correlation and time lag, to the observations than the control run.

At Bideford, in the Bristol Channel, the cross correlation between the wave parameter modulations and the sea surface height modulations is also significantly greater for the observations than for the wave model. Again, this indicates that the model is not able to fully represent the effect of the tide at this location. The tidal range is large at Bideford (approx 8m) suggesting that the absence of water level changes in the model is likely to be the reason for this. Nevertheless, there is an increase in the maximum correlation for the model with currents, implying that the addition of a current field has had a positive impact on the model performance. A significant lag exists between the wave parameter modulations and the sea surface height, suggesting the dominant processes at this location may be different from those in the area surrounding the Isle of Wight. The lag for the model with currents is more consistent with the observations than for the control run.

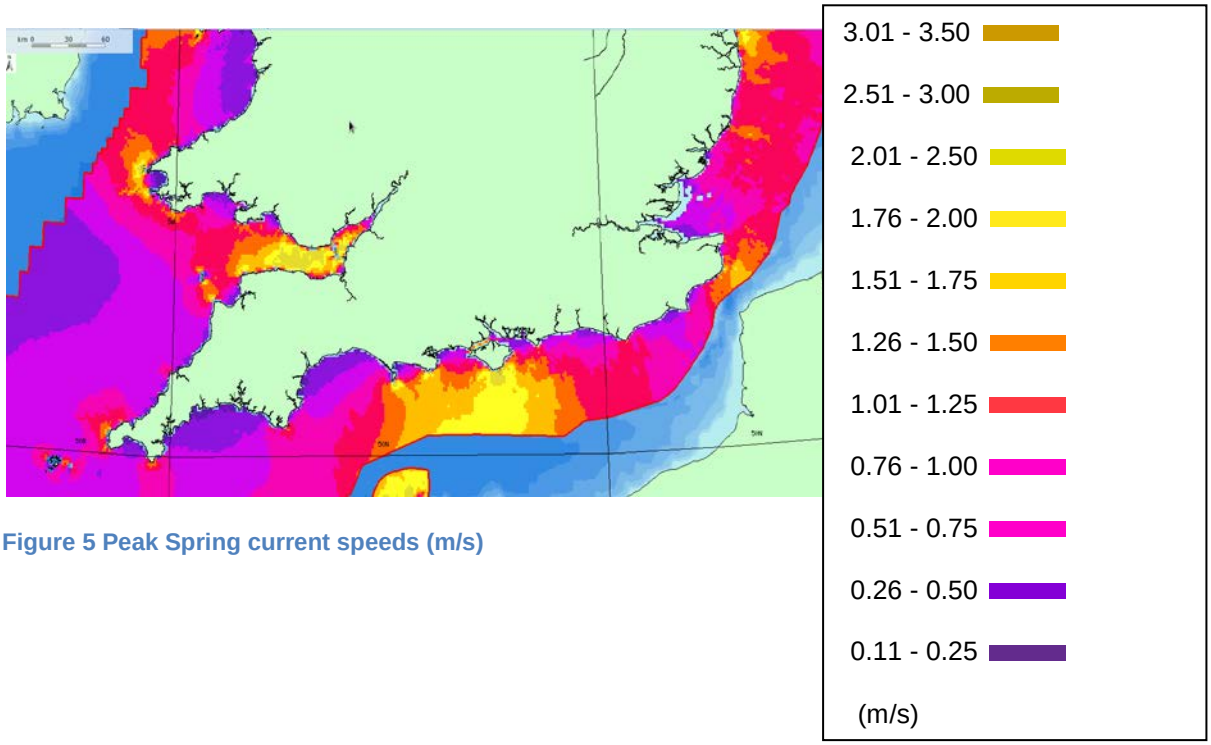

Figure 5 Peak Spring current speeds (m/s)

Taken from Atlas of UK Marine Renewable Energy Resources. 2008. ABPmer. (. 29 October 2015) http://www.renewables-atlas.info/

3.2 Case studies

3.2.1 Rustington: 6th -13th February 2012

Power series derived from the wavelet analysis identified a number of time periods where the currents had a dominant impact on the wave field.. This case study approach also allows the local wave-current processes to be investigated in more detail.

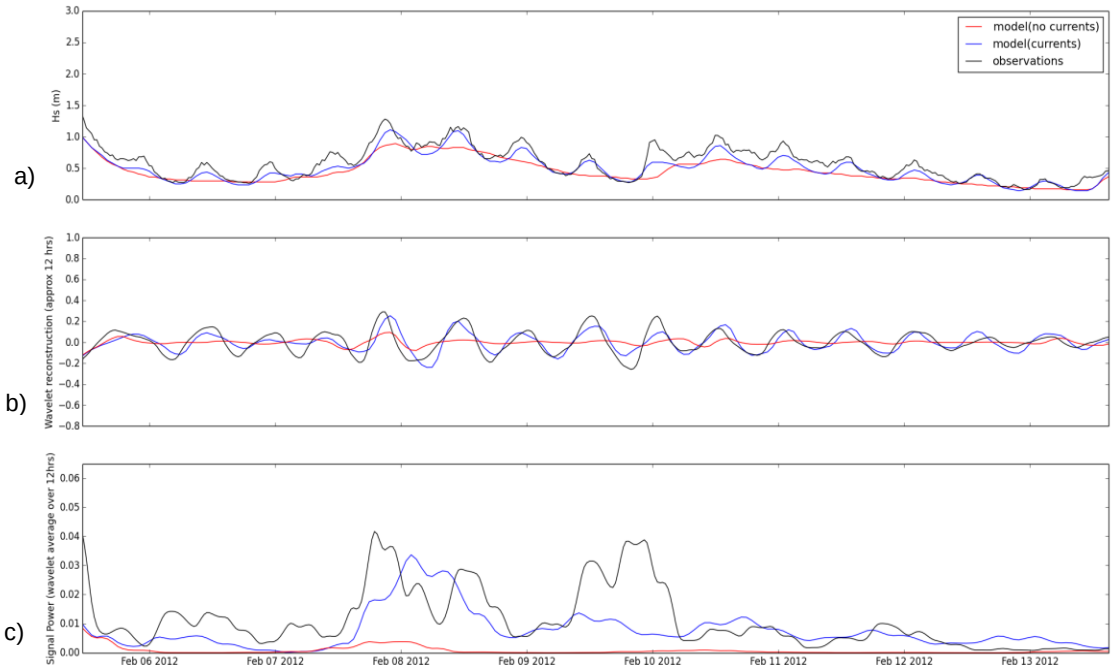

Figure 6a) Hs time series at Rustington b) Wavelet reconstruction for an approximately 12 hour period c) The signal power of the reconstruction averaged over a 12 hour window

A case study that was identified from the records at Rustington was the period of the 6th to the 13th February 2012. The Hs time series for the observations, model with currents and the control run is shown in figure 6, along with the 12hr wavelet reconstruction (figure 6b). The main wave parameters during this time period are shown in figure 7. The difference in the signal power between the model with currents and the control run is evident. Hs and Tz (figure 7a and b) show strong modulations, these are approximately in phase with the sea surface height for the model with currents and the observations, which are absent in the control run. There are also significant modulations in the directional spread (figure 7c), which indicate that tidal effects are causing changes in the wave refraction locally at Rustington.

The peak period (Tp) and peak wave direction record for the wave buoy at Rustington (figure 7d), shows regular large fluctuations. The sharp increase in Tp, along with the change in direction of over 100°, is due to a bimodal wave spectrum comprising two different sources of wave energy. One component comprises swell waves propagating toward the northeast from the Atlantic and the other is locally wind generated waves from an easterly direction

(propagating westward). The presence of a bimodal sea means that, in order to better understand the processes causing variations in the wave parameters, it is necessary to look at the wave spectrum. The sudden large changes in the Tp for the total spectrum indicate that peak energy in the spectrum is switching periodically from the wind-sea to the swell.

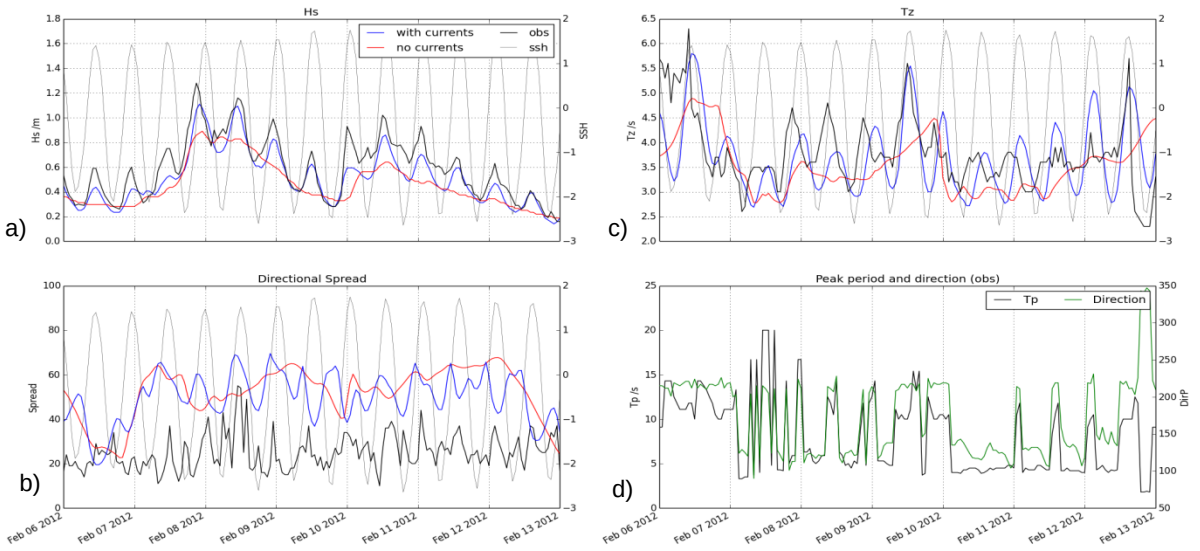

Figure 7 Time series at Rustington for Observations and Models. a) Hs b) Tz c) Directional spread d) Tp

The frequency spectrum from the wave buoy confirms that the fluctuations in the Tp are being caused by periodic increases in the swell wave energy (figure 8a) and b). It was found that there was a significant increase in swell wave energy at the high tide, while the wind-sea energy had relatively little change. It is this increase in the swell energy rather than a reduction in the wind-sea that causes the shift in Tp seen in figure 7d.

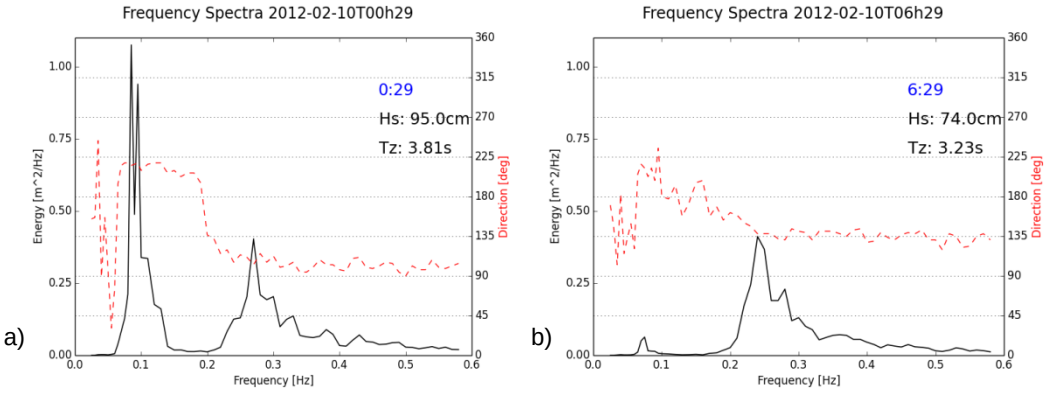

Figure 8 a) Frequency Spectrum at Rustington at high tide b) low tide.

The model spectra for the same time period show the same increase in swell energy at high tide (figure 9). The directional wave spectra from the model also show that this increase in energy is related to an increase in the directional spread. This suggests that a change in the wave refraction is increasing the swell energy locally at Rustington. The hindcast carried out

without a model field does not show this change in the swell part of the wave spectrum (figure 9b.) The wave spectrum at low tide for the control model is shown in figure 10a) and the spectrum for the model with currents in figure 10b). If these are compared with figure 9 a) and b) it can be seen that there is little change in the swell over the 6 hour period for the control model. For the model with currents however, there is a reduction in swell energy and a change in the direction spread. The wave field for the model with currents also shows refraction of the swell by currents during the tidal cycle. A following current (rising tide) refracts swell waves towards the coast causing the waves to refract towards Rustington increasing the swell energy and directional spread. There is a gradient in current speed from the coast to the deeper water, in a following current the waves in the deeper water are travelling faster than those closer to the coast. This leads to refraction towards the coast. In an opposing the current, the waves in the deeper water where current speeds are faster, travel slower. This causes them to be refracted away from the coast. The refraction of swell energy towards Rustington peaks at or near high tide. A counter current (ebbing tide) causes swell to be refracted away from the coast.

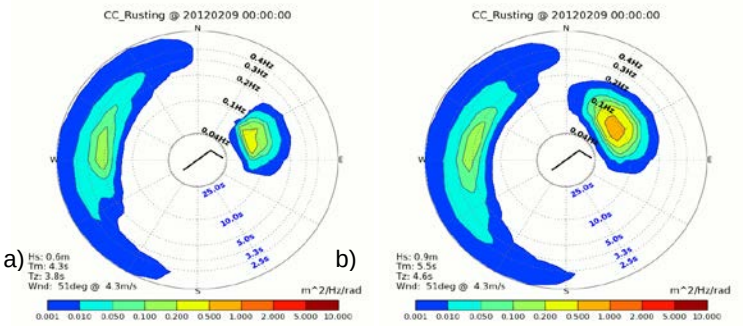

Figure 9 Directional wave spectrum at Rustington at high tide a) Model without currents b) Model with currents

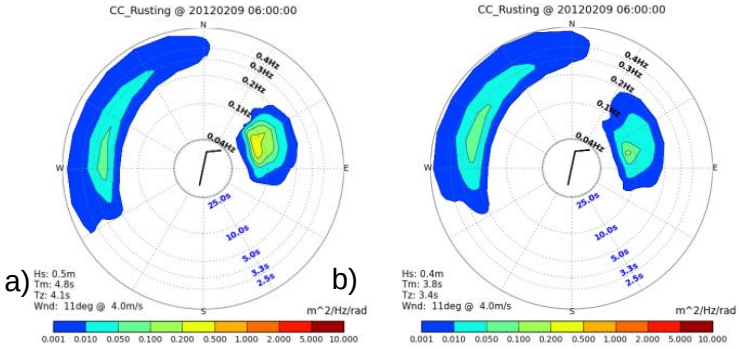

Figure 10 Directional wave spectrum at Rustington at low tide a) Model without currents b) Model with currents

During the time period of this case study the RMSE was calculated at Rustington for both model runs. When currents were added to the model there was a decrease in the RMSE from 0.18m to 0.15m. This is a significant improvement in the relative error at this location.

3.2.2 Bideford: 21st-22nd March 2012

The wavelet analysis was used to identify a case study at Bideford for 21st-22nd of March 2012. At Bideford the signal power in the 12hr wavelet is significantly greater for the observations than for the wave model with a current field (see figure 11). At this location there is only a small difference between the control run and the model run with a current field (figure 12). This suggests that the modulations in the wave parameters observed at the wave buoy are caused by additional processes to changes in current speed and direction. The changes in water depth due to the tide have not yet been added to the wave model. Therefore changes in depth related dissipation and refraction are not accounted for. As can be seen in figure 12 the maximum tidal range during the period of this case study is just over 8m at Bideford almost double the range at Rustington (figure 5) Depth changes may therefore be more significant at Bideford. The observed wave parameters for Bideford are shown in figure 13. Figure 13d), shows that the observed Tp varied between 10 and 12.5 seconds during the time period. This along with low wind speeds (figure 13e) is an indication that the sea state was swell dominated during this case study. The frequency spectra are available for the Bideford wave buoy and this confirms that the wave energy during this case study was predominantly swell (figure 14).

The swell energy is greatest at, or within an hour either side of low tide (figure 14) at 0:600 and 18:00 respectively. The directional spread increases at high tide (figure 13c) and decreases as the swell energy increases at low tide. The swell energy is at a minimum at low tide or within an hour of the low tide. At Rustington an increase in swell energy was seen in the wave spectra at high tide and with an increase in directional spread. This suggests that the processes affecting the swell at Bideford are different and probably largely related to depth changes rather than current refraction of the swell. It is possible that depth changes are causing the focussing of swell energy towards the coast at Bideford but this not clear from this study. The addition of tidal elevations to the wave model may help determine the processes occurring at Bideford. It is likely that this will also improve the performance of the wave model at this location.

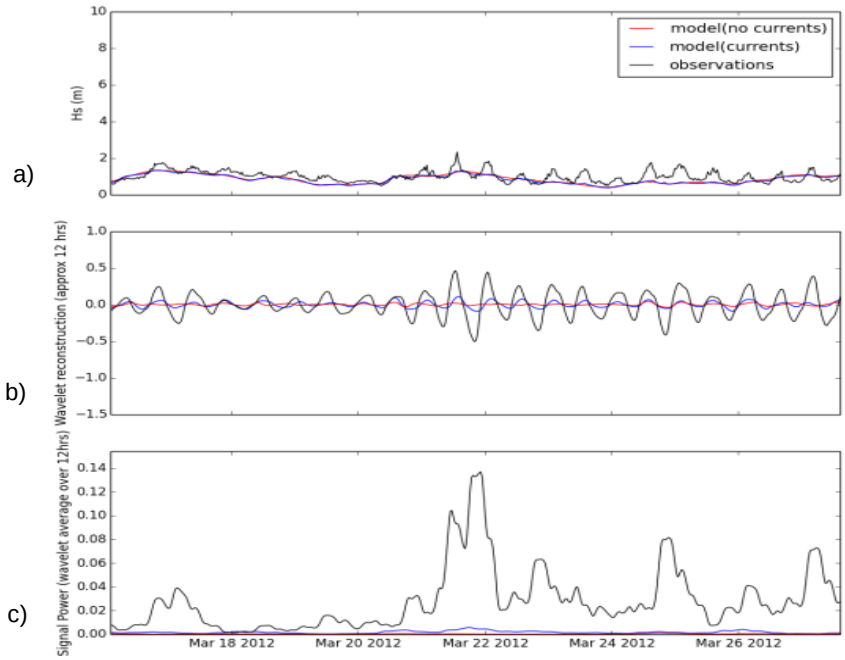

Figure 11 a) Hs time series at Bideford b) Wavelet reconstruction for an approximately 12 hour period c) The signal power of the reconstruction averaged over a 12 hour window

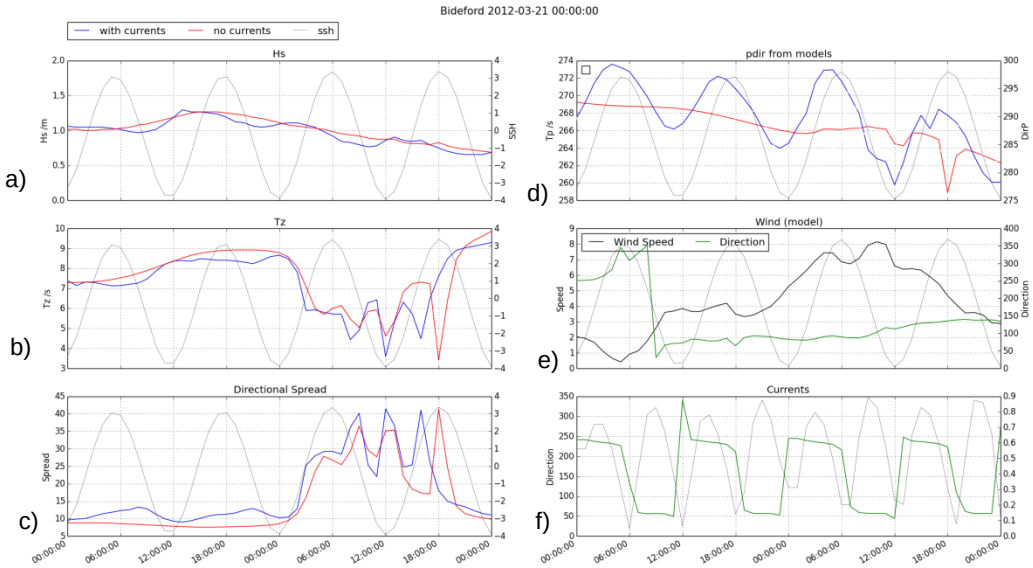

Figure12 Time series of model with currents and model without currents a) Hs b)Tz c) Directional Spread d) Tp and peak direction e) wind speed and direction f) current speed and direction

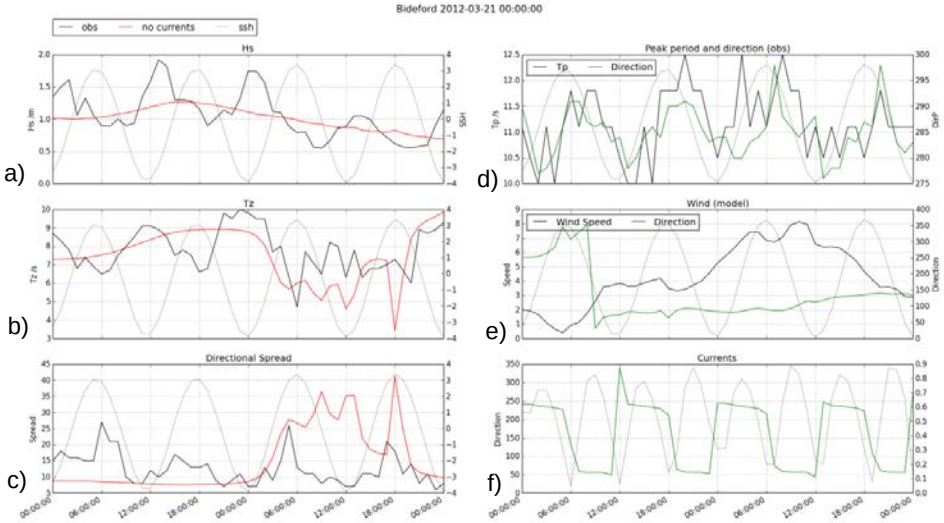

Figure 13 Time series of observations and model without currents a) Hs b)Tz c) Directional Spread d) Tp and peak direction e) wind speed and direction f) current speed and direction.

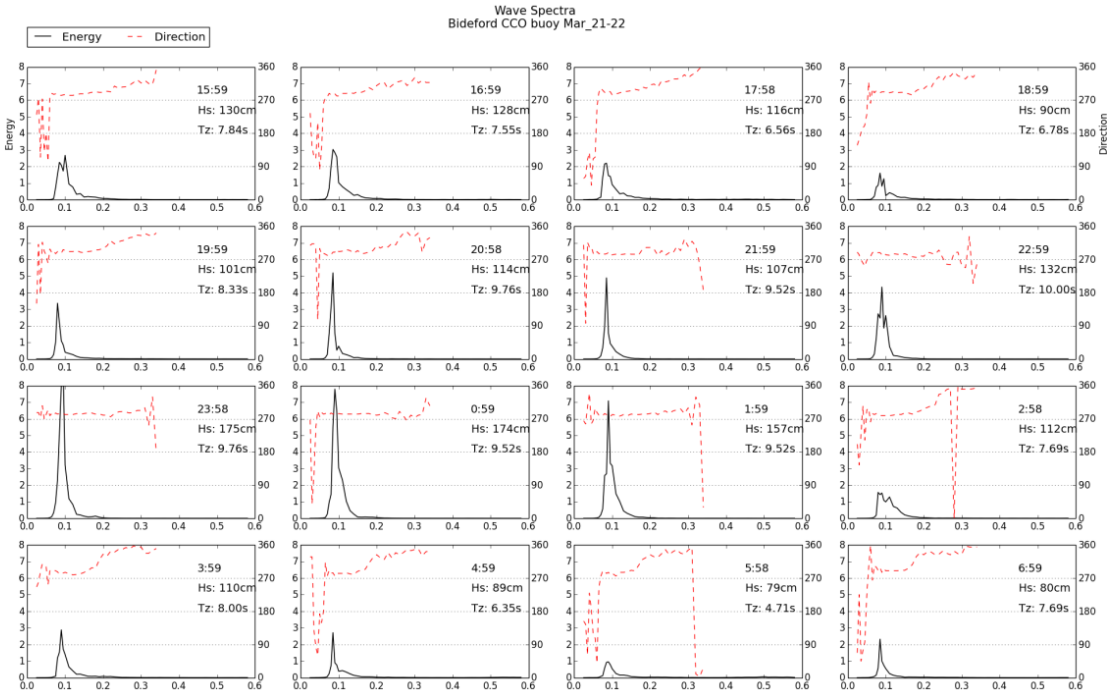

Figure 14 Series of frequency spectra at Bideford on March 21st -22nd

4. Summary and Conclusions

A discrete wavelet analysis has been used to successfully indentify suitable case studies for the validation of wave-current interaction in a one way coupled model. A 12 hour tidal signal can be isolated from a wave parameter time series using a suitable wavelet function. A model run without currents has been successfully used as a control dataset to identify where 12 hour modulations may occur in the time series without the presence of tidal currents. Once these time periods are excluded the influence of tidal currents can be identified from the power in the 12 hour signal in the observations and the output from a model which includes a current field.

Comparison of the (lagged) correlation between the wavelet band pass filter (12 hour period) with processes such as the sea surface height can help to improve understanding of how different tidal processes affect the wave field at different locations. In this study, a large difference in correlation between the observations and the wave model can probably be attributed to the wave model not representing processes related to tidal elevation changes.

Two different locations have been investigated, one where the effects of wave-current interaction were largely responsible for the modulations observed in the wave parameter time series and one where the changes in tidal elevations are likely to have had a larger effect on the wave field. At Rustington the addition of a current field to the wave model improved the performance of the model; it also resulted in an approximately 15% improvement in the RMSE. Locally the effect of current refraction was found to affect the swell energy that propagated to the buoy location. A comparison of the wave buoy and model spectra showed that when a current field was added to the wave model it was better able to represent the behaviour of the observed wave spectrum.

At Bideford large variations in water depth associated with the tide are believed to significantly impact waves at the site. Therefore, adding a current field to the wave model, only partly represented tidal variability. The addition of tidal elevations to the wave model is planned as part of ongoing work to improve the performance of the UK wave model.

5. References

Arhuin, Fabrice. “Dissipation parameterizations in spectral wave models and general suggestions for improving on today’s wave models.” ECMWF Workshop on "Ocean Waves" - 25 to 27 June 2012. Proceedings: http://old.ecmwf.int/publications/library/do/references/list/201210251

Ardhuin, Fabrice, Aron Roland, Franck Dumas, Anne-Claire Bennis, Alexei Sentchev, Philippe Forget, Judith Wolf, Françoise Girard, Pedro Osuna, and Michel Benoit. "Numerical wave modeling in conditions with strong currents: Dissipation, refraction, and relative wind." Journal of Physical Oceanography 42, no. 12 (2012): 2101-2120.

Daubechies, Ingrid. "The wavelet transform, time-frequency localization and signal analysis." Information Theory, IEEE Transactions on 36.5 (1990): 961-1005.

Dodet, Guillaume, Xavier Bertin, Nicolas Bruneau, André B. Fortunato, Alphonse Nahon, and Aron Roland. "Wave-current interactions in a wave-dominated tidal inlet." Journal of Geophysical Research: Oceans 118, no. 3 (2013): 1587-1605.

Flather, R. A.: A tidal model of the northwest European continental shelf, Memoires de la Societe Royale de Sciences de Liege, 6, 141–164, 1976.

Hayes, John G. "Ocean current wave interaction study." Journal of Geophysical Research: Oceans (1978–2012) 85.C9 (1980): 5025-5031.

Holthuijsen, L. H., and H. L. Tolman. "Effects of the Gulf Stream on ocean waves." Journal of Geophysical Research 96.C7 (1991): 12-755.

Holthuijsen, Leo H. Waves in oceanic and coastal waters. Cambridge University Press, 2007.

Kunze, Eric. "Near-inertial wave propagation in geostrophic shear." Journal of Physical Oceanography 15.5 (1985): 544-565.

Li, Jian-Guo. "Upstream nonoscillatory advection schemes." Monthly Weather Review 136.12 (2008): 4709-4729.

Longuet-Higgins, Michael S., and R_W Stewart. "Changes in the form of short gravity waves on long waves and tidal currents." Journal of Fluid Mechanics 8.04 (1960): 565-583.

Longuet-Higgins, Michael S., and R. W. Stewart. "Radiation stresses in water waves; a physical discussion, with applications." Deep Sea Research and Oceanographic Abstracts. Vol. 11. No. 4. Elsevier, 1964.

O'Dea, E. J., A. K. Arnold, K. P. Edwards, R. Furner, P. Hyder, M. J. Martin, J. R. Siddorn et al. "An operational ocean forecast system incorporating NEMO and SST data assimilation for the tidally driven European North-West shelf." Journal of Operational Oceanography 5, no. 1 (2012): 3-17

Schumann, E. H., High waves in the Agulhas current, The South African Shipping News and Fishing Industry Review, 25–27, 1975.

Schumann, E. H., High waves in the Agulhas current, Mariners Weather Log, 20, 1976.

Tolman, Hendrik L. "The influence of unsteady depths and currents of tides on wind-wave propagation in shelf seas." Journal of Physical Oceanography 20.8 (1990): 1166-1174.

Tolman, Hendrik L. "A third-generation model for wind waves on slowly varying, unsteady, and inhomogeneous depths and currents." Journal of Physical Oceanography 21.6 (1991): 782-797.

Tolman, Hendrik L. "User manual and system documentation of WAVEWATCH III TM version 3.14." Technical note, MMAB Contribution 276 (2009).

Torrence, Christopher, and Gilbert P. Compo. "A practical guide to wavelet analysis." Bulletin of the American Meteorological society 79.1 (1998): 61-78.